

**Ventilation for Energy Efficiency and Optimum  
Indoor Air Quality  
13th AIVC Conference, Nice, France  
15-18 September 1992**

**Paper 24**

**Simulation of Gas Leaks in Ventilated Rooms**

**E. Cafaro<sup>\*</sup>, N. Cardinale<sup>\*\*</sup>, G.V. Fracastoro<sup>\*</sup>, E.  
Nino<sup>\*\*</sup>, R.M. Di Tommaso<sup>\*\*</sup>**

**\* Dipartimento di Energetica del Politecnico di  
Torino, Corso Duca degli Abruzzi 24, 10129 Torino,  
Italy**

**\*\* Dipartimento di Ingegneria e Fisica  
dell'Ambiente, Universita della Basilicata, Via  
N.Sauro, 85 - 85100 Potenza, Italy**

## SIMULATION OF GAS LEAKS IN VENTILATED ROOMS

E. Cafaro (\*), N. Cardinale (\*\*), G.V. Fracastoro (\*), E. Nino (\*\*), and R.M. Di Tommaso (\*\*)

(\*) Dipartimento di Energetica del Politecnico di Torino, Corso Duca degli Abruzzi, 24 - 10129 TORINO (Italy).

(\*\*) Dipartimento di Ingegneria e Fisica dell'Ambiente, Università della Basilicata, Via N. Sauro, 85 - 85100 POTENZA (Italy).

### SYNOPSIS

The study deals with the theoretical and experimental simulation of gas leaks in buildings. Such simulations may provide helpful information about the flow characteristics and dangerous concentrations as a function of the ventilation system (if any), the geometrical features and the thermal constraints on the room, and eventually about the positioning of gas monitoring devices.

Theoretical simulations are performed using a three-dimensional, finite volume CFD package in order to provide the velocity, temperature and concentration fields in a room. Experimental simulations have been performed in the full-scale ventilation test room at the University of Basilicata.

### 1. Introduction

The paper is concerned with a particular case of contaminant diffusion indoors, related with natural gas leaks, the consequences of which may be dramatic if concentrations above 5-6 % are reached [1]. The correct positioning of gas leak detectors is of paramount importance, and requires a detailed knowledge of gas diffusion within the building. The influence on gas diffusion paths of ventilation systems, rooms geometry and thermal conditions on one side, and gas leak flow characteristics on the other side has to be thoroughly investigated.

The philosophy of this study was to carry on both a theoretical and an experimental evaluation of the phenomenon. The experimental part of the study was performed using a full-scale test room, the so-called CVC (Controlled Ventilation Chamber) of the University of Basilicata. In the CVC the experiments were performed using  $N_2O$  and  $SF_6$ , while  $CH_4$  is being used only recently.

The theoretical simulations were carried on at Turin Polytechnic: among the growing number of computer codes existing in this research field [2], the Create Inc. FLUENT package has been chosen, because of its reliability in predicting contaminant diffusion indoors and outdoors. A validation of FLUENT package has already been performed recently, with fair results [3].

In a first phase of the work the code was used to simulate the non-uniform decay of concentration of a tracer gas, while more recently the concentration increase with time has been investigated. In both cases, the main parameter was assumed to be the ventilation strategy, in terms of number of air changes and positioning of inlets/outlets.

Results were obtained in terms of both concentration and velocity fields, but particular attention has here been devoted to concentrations.

## 2. The experimental apparatus

The description of CVC was the aim of previous papers [4], [5], to which the reader is sent back for more information.

The CVC has a volume of 17 m<sup>3</sup> and allows balanced, immission or extraction ventilation, with air entering or being extracted from up to four grilles, located on two opposite vertical walls, and ventilation rate ranging between 0 and 10 ach. Instrumentation includes a three-cell Gas Analyzer (SF<sub>6</sub>, NO<sub>2</sub>, and CH<sub>4</sub>), six non-directional hot film anemometers working in the range from 0 to 0.5 m/s, a flowmeter for the measurement of air flow rate to the CVC, and two computer driven, automatic systems, one for establishing the air sampling sequence across six ducts, and the second for moving the air sampling ducts and the velocity sensors around the test room.

## 3. The main features of the CFD package

A turbulent flow in isothermal conditions and in the presence of a pollutant source, as in this set of tests, can be modelled by the Reynolds-averaged equations for mass, momentum (Navier-Stokes equation), and concentration, and the state equation for the fluid.

The above set of equations do not represent a closed system because the viscous stresses depend in their turn on the fluctuating components of the velocity vectors, which are unknown.

The "closure" of the system requires the introduction of a suitable turbulence model, i e, to express the components of the Reynolds stress tensor as a function of known, equivalent time-averaged quantities.

Different options exist for turbulence modelling: FLUENT package offers a two-equation k-ε Model for high Reynolds number and an Algebraic Stress Model.

The k-ε Model is generally, but not universally believed to be the appropriate level of turbulence model for air flow in buildings. However, for certain situations the limitations due to assuming isotropic turbulence may prove to be inadequate: an Algebraic Stress Model may be adopted although the increased computing time may prove prohibitive. The computational overload of an Algebraic Stress Model is found to be approximately 100 %.

The set of seven non-linear partial differential equations involved in the CFD model may be represented by the single prototype equation:

$$\frac{\partial(\rho \phi)}{\partial t} + \frac{\partial}{\partial x_i} (\bar{\rho} \bar{u}_i \phi - \Gamma_\phi \frac{\partial \phi}{\partial x_i}) - S_\phi = 0$$

where

- ϕ = main variable
- Γ<sub>ϕ</sub> = exchange coefficient
- S<sub>ϕ</sub> = source term for the main variable

The meaning of the generalized symbols for each equation is given in Table I.

The values of the coefficients in the k-ε model are standardized for most engineering flows, but are not universal constants for any turbulent flow. The present calculations are performed using the standard values

which may be found in the literature [6].

The airflow model field equations in the FLUENT package are expressed in time-implicit and conservative finite difference form on a staggered grid, and solved using the SIMPLE pressure correction algorithm: two variants, namely the SIMPLEC and the PISO algorithms are also available. The variants are claimed to improve the rate of convergence. Selecting the PISO algorithm a slight increase in the size of the used computer memory appears. Underrelaxation is used to promote stability and convergence: the right selection of the underrelaxation parameters is of paramount importance for a correct solution.

The SIMPLE scheme is strongly elliptic with unitary ellipticity measure, which characterizes the amplification of errors in the high wave number modes: energy cannot accumulate in the grid scale wave number component and the occurrence of the grid scale pressure oscillation is prevented. Additionally, the use of a finite volume discretization ensures the integrability of the SIMPLE scheme.

Two differencing schemes are available, namely, a "hybrid" scheme and the Quadratic Up-Stream Interpolation for Convective Kinematics (QUICK).

The mathematical model has to be completed with suitable initial and boundary conditions. For this specific problem the following conditions were assumed:

- at the inlet cells: the distribution of air velocity, of turbulent kinetic energy, and of turbulent kinetic energy dissipation rate for the ventilation air and the leaking gas;
- at the outlet cells: the longitudinal component of the velocity vector, calculated making use of the equation of continuity;
- at the walls: the gradients of the main variable are assumed zero; suitable "wall functions" are used for the determination of the parallel components of velocity vectors.

The initial turbulent kinetic energy has been calculated by means of the relation:

$$k_0 = (3/2) \cdot I^2 \cdot U_0^2$$

where

I = non-dimensional turbulence intensity, assumed equal to 0.15

$U_0$  = mean value of the velocity vector at the inlet

The initial dissipation rate has been calculated by the following equation:

$$\epsilon_0 = k_0^{1.5} / (\alpha H)$$

where

H = characteristic dimension of the system

$\alpha$  = suitable numerical coefficient

To the domain of calculation a non-uniform cartesian grid including 22x44x8 cells has been superposed. The simulation has been performed in a three-dimensional domain and adopting a symmetry plane in longitudinal direction. It should be stressed that the solution is not grid-independent, while the adoption of different values of  $k_0$  and  $\epsilon_0$  does not seem to produce relevant variations in the calculations.

Simulations have been performed on two PC IBM compatible 80386 and 80486, and a workstation HP 720 Apollo. The running time ranged from about 48 hours for the 80386 to 8 hours for the Apollo.

#### 4. Comparison of theoretical and experimental results

A complete scheme of the experimental tests performed both for the concentration decay and for the concentration growth with time is shown in Table II.

Theoretical simulations were mainly dealing with decay analysis using  $SF_6$  and  $N_2O$ , and growth analysis using  $SF_6$  and  $CH_4$ .

The main problem in comparing the results is that the outputs are not homogeneous, that is:

- while the numerical results are known at fixed time steps (usually of five minutes), the experimental results are continuous

- while the numerical results are known at a number of locations varying between 15,500 and 50,000, the experimental data are collected only at five locations simultaneously, along a vertical rod, plus the exhaust. In order to multiply the number of points, measurements were repeated, trying to reproduce exactly the same experimental conditions, and moving the vertical rod around the CVC. Fig. 1 illustrates the position of measurement points on the CVC plan.

In order to verify the repeatability of experiments, the concentration at the exhaust was adopted as primary key. For example, for case B1, shown in Fig. 2, concentrations at the exhaust were confined within a band of 10 - 20 ppm, corresponding to 5 - 10 %. On the same graph the computed value is shown: this appears underestimated during the first 15', then falls beneath the band of measured values and appears slightly overestimated at the end of the 30' period.

Fig. 3 reports the volume of tracer gas removed from the CVC with time, given by the integral of the concentration-volume air flow product. In this case the theoretical and experimental results are very close one to the other (3-4 %). This parameter seems more reliable than instantaneous values, which are subject to random errors.

The comparisons are carried on for the decay cases B1, B3, C3, and for the growth case B1, and will be shown in terms of concentration fields.

The results are shown for some of the points on the plan of CVC shown in Fig. 1, adopting the height above the floor as a parameter. Fig. 4 and 5 illustrate respectively the measured and computed values for case B1 at the room centre (point 0), as an example. Errors keep in a 10 % range at any time below 0.80 m and at the exhaust, but may rise to 80-90 % at points above 1.50 m, after the first 20'.

Fig. 6 shows the ventilation efficiency for case B1, defined as the ratio between concentrations at the exhaust and at the considered point, calculated and measured at three different heights at point 1.

Figs. 7 and 8 show the concentration fields after 10' for cases B3 and C3. It should be observed that case C3 provides a much better result, without stagnancy situations as for case B3.

Figs. 9 and 10 show the velocity fields for cases B3 and B1. They present an interesting phenomenon, which could not be easily predicted: in the first case the air creeps along the floor until it reaches the opposite wall, while in case B1, due to the low horizontal component of velocity and the density difference between clean air and air with tracer gas ( $SF_6$ ), it climbs along the wall where the outlet grille is positioned under the action of a sort of "stack effect".

Finally, Figs. 11 and 12 show the measured and calculated "concentration growth" for case B1. It appears evident, from the comparison, that the actual distribution of concentration is, at least in the first 30', much more uniform than the calculated one. However, the concentrations at the exhaust - termed "sc" in both Figures - are quite similar and end with

exactly the same value (120 ppm). After the first 30' the expected SF<sub>6</sub> stratification appears also in the experimental results.

## 5. Conclusions and future developments

Although the comparisons are limited to a small number of cases and the experimental procedure still needs some adjustment, some conclusions may already be drawn for the "decay" tests:

- in general there is a fair qualitative agreement between measured and calculated concentration values both for space and time variations;
- for the decay tests, the difference between measured and calculated data tends to increase with time, as could be expected, due to the uniformity of initial concentration. It also systematically increases with height.

For the "growth" cases, the concentration time trends show a fair agreement, while the calculated space variations appear overestimated.

Future developments include, in the experimental part of the work, the completion of measurement campaigns using CH<sub>4</sub>, and the execution of visualization tests by means of a reduced-scale physical model, already realized at the Department of Energetics.

Future developments of the theoretical part of the work include the use of Algebraic Stress Models, and the adoption of Body Fitted Coordinate system in order to improve the meshing of the region at the supply opening.

## 6. Acknowledgements

The research was funded by the Italian Ministry for University and Scientific Research MURST 60 %, under the program "Controlled ventilation within confined spaces", coordinated by G.V. Fracastoro. The authors wish to express their gratitude to C. Cima and M. Perino for their skillful and patient assistance in the calculation phase, and to F. Mariniello for his assistance in the measurement campaigns.

## 7. References

- [1] Harris, R.J., *The investigation and control of gas explosions in buildings and heating plant*, British Gas, E & FN Spon, London, New York.
- [2] Liddament, M.W., *A Review of Building Air flow Simulation*. AIVC, Technical Note 33, March 1991.
- [3] Cafaro, E., Fracastoro, G.V., Nino, E., Perino, M., *Analisi teorico-sperimentale della diffusione degli inquinanti negli ambienti confinati*, Atti del 46° Congresso nazionale A.T.I., Cassino-Gaeta, 25-27 settembre 1991.
- [4] Fracastoro, G.V., Nino, E., and Coretti, G., *The Ventilation Chamber of the University of Basilicata*, Proc. 11th AIVC Conference, Belgirate (Italy), 1990.
- [5] Fracastoro, G.V., Nino E., *La Camera a Ventilazione Controllata*

dell'Università della Basilicata, Convegno AICARR, Roma, Aprile 1991.

[6] Patankar, S.V., *Numerical Heat Transfer and Fluid Flow*, Hemisphere Publishing Co., 1980.

Table I  
Meaning of the symbols in the prototype equation.

Equation	Principal variable $\phi$	Exchange coefficient $\Gamma_{\phi}$	'Source' term $S_{\phi}$
Momentum	$\bar{u}_i$	$\mu_{eff}$	$\bar{\rho} \bar{X}_i + \frac{\partial}{\partial x_j} \left[ \mu_{eff} \left( \frac{\partial \bar{u}_j}{\partial x_i} - \frac{2}{3} \frac{\partial \bar{u}_k}{\partial x_k} \delta_{ij} \right) \right] - \frac{\partial \bar{p}}{\partial x_i}$
Continuity	1	0	0
Turbulence energy	$k$	$\frac{\mu_t}{\sigma_k}$	$\mu_t C_1 - \rho \epsilon$
Energy dissipation	$\epsilon$	$\frac{\mu_t}{\sigma_{\epsilon}}$	$\frac{\epsilon}{k} (C_1 \mu_t G - C_2 \rho \epsilon)$

Table II  
List and features of experimental tests.

Test	Air changes	Vent. strategy	Conc./No.pnts.	Vel./No.pnts.
(1)				
Decay				
A1	1	A	5x1+exhaust	No
B1	1	B	5x12+exhaust	No
C1	1	C	5x1+exhaust	No
D1	1	D	5x1+exhaust	No
E1	1	E	5x1+exhaust	No
A1.5	1.5	A	5x1+exhaust	No
B1.5	1.5	B	5x1+exhaust	No
C1.5	1.5	C	5x1+exhaust	No
D1.5	1.5	D	5x1+exhaust	No
E1.5	1.5	E	5x1+exhaust	No
A2	2	A	5x1+exhaust	No
B2	2	B	5x1+exhaust	No
C2	2	C	5x1+exhaust	No
D2	2	D	5x1+exhaust	No
E2	2	E	5x1+exhaust	No
B3	3	B	5x9+exhaust	6x30
C3	3	C	5x1+exhaust	6x30
Growth				
A1	1	A	5x3	No
B1	1	B	5x3	No
C1	1	C	5x3	No
D1	1	D	5x3	No
E1	1	E	5x3	No

- (1) A = inlet down(D)/right(R), outlet D/left(L)  
 B = inlet D/R, outlet up(U)/L  
 C = inlet D/R, outlet U/R  
 D = inlets D/R, outlets U/R + U/L  
 E = inlets D/R + U/L, outlets D/L + U/R

### Fig. 1 – CVC Plan

Measurement points

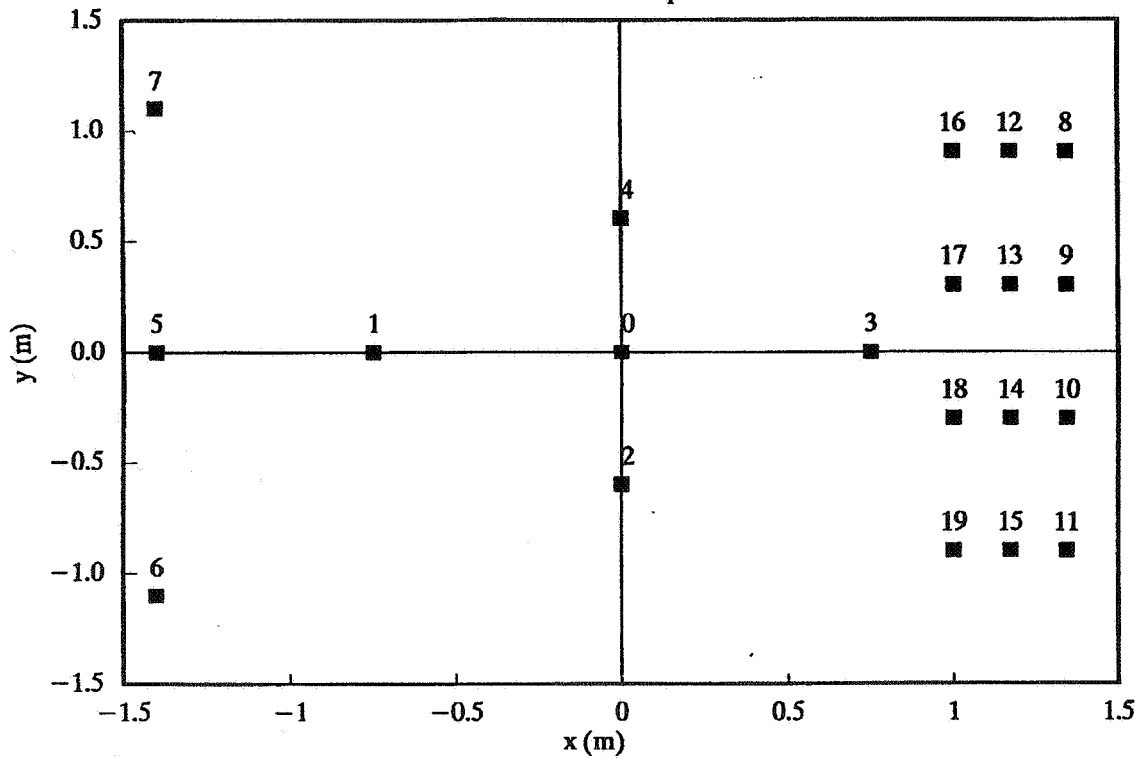
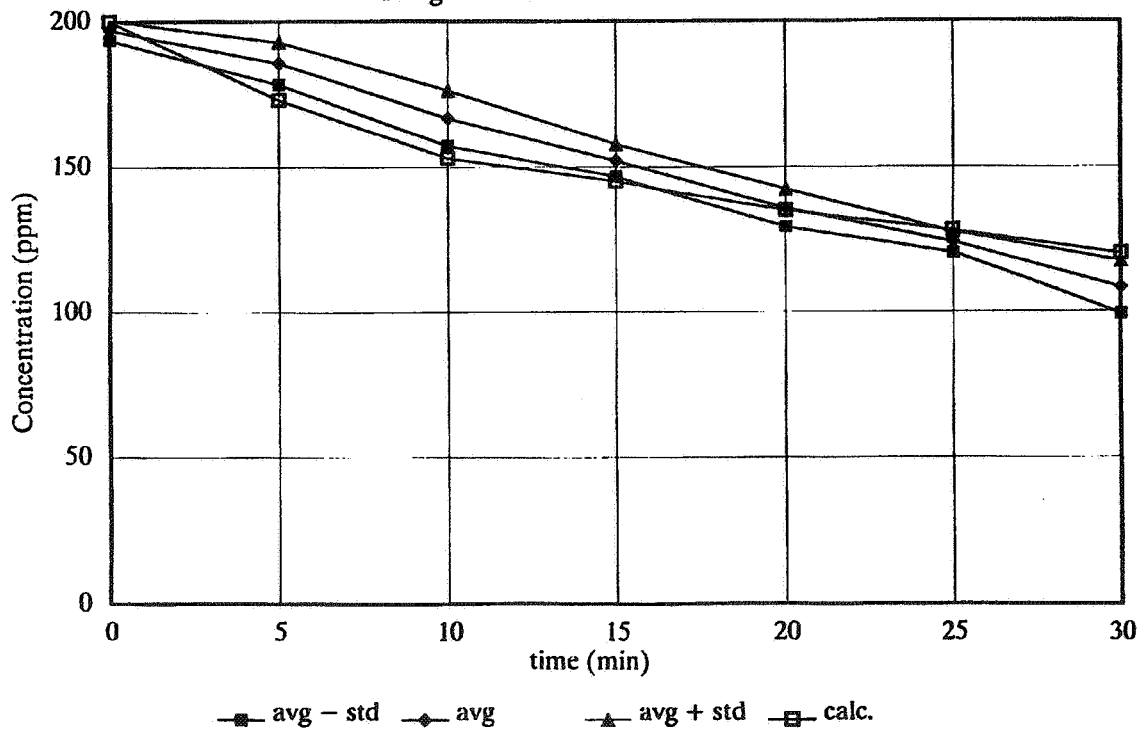


### Fig. 2 – Concentration at the exhaust

Range of measured and calculated values

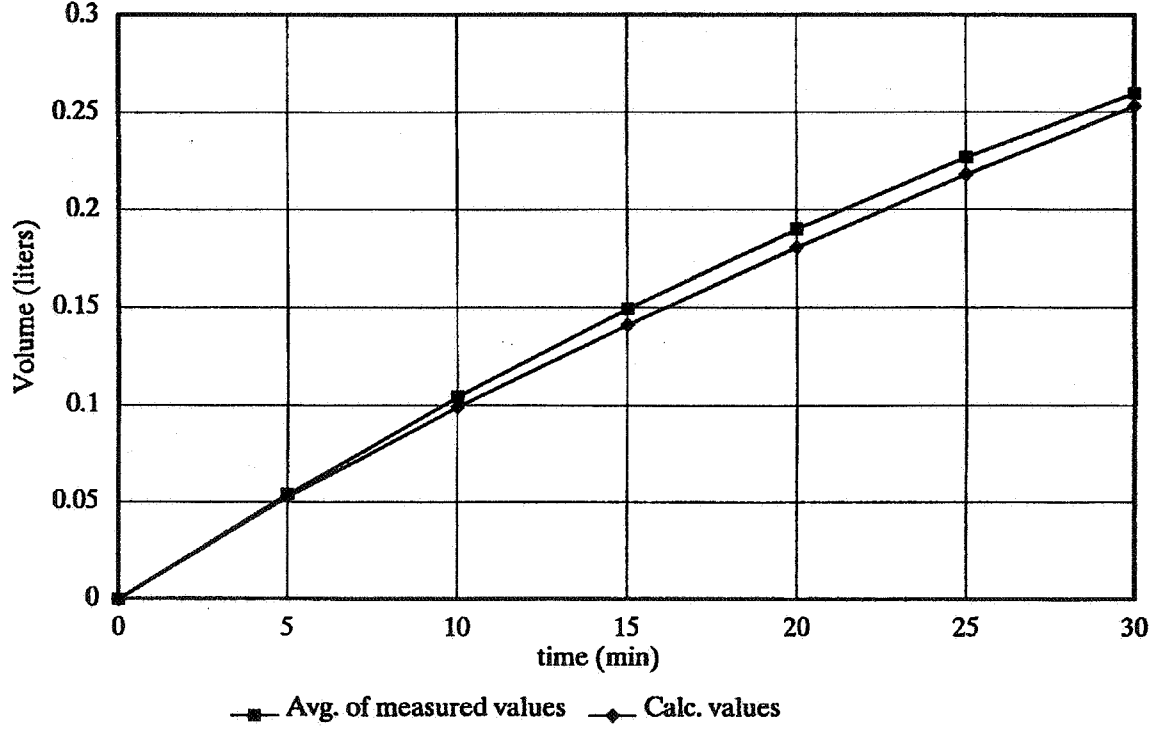


Case B1



**Fig. 3 – Volume of removed tracer gas**

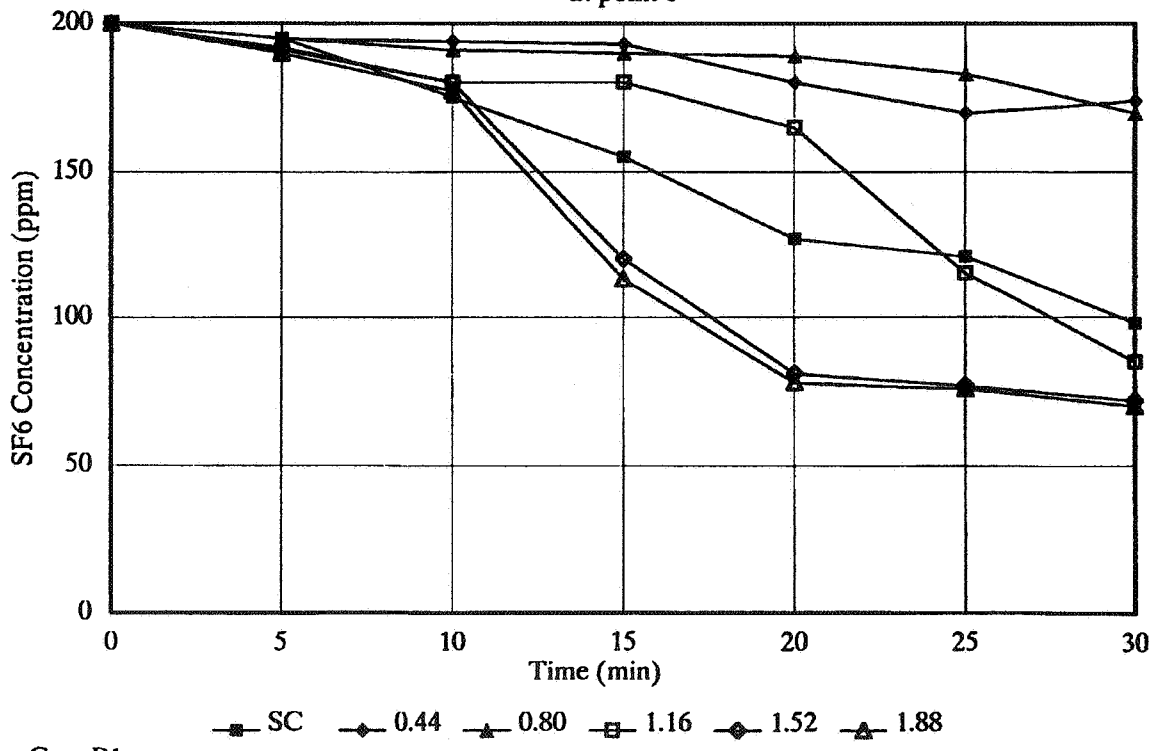
Calculated and measured values



Case B1

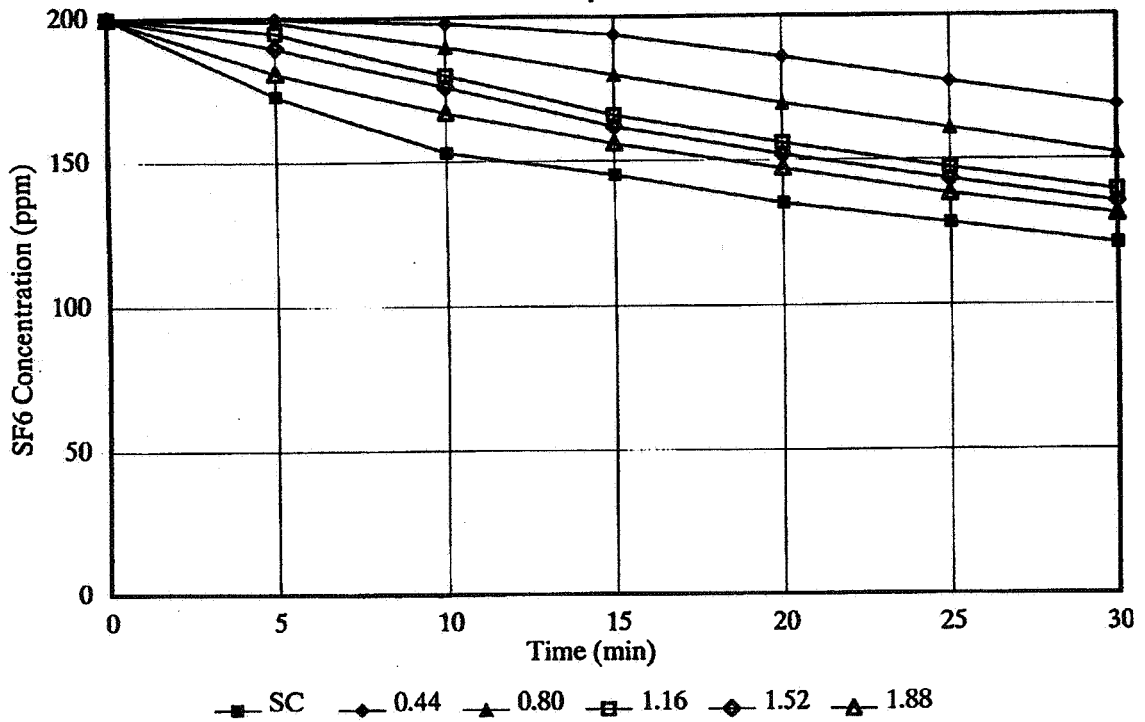
**Fig. 4 – Measured Concentration decay**

at point 0



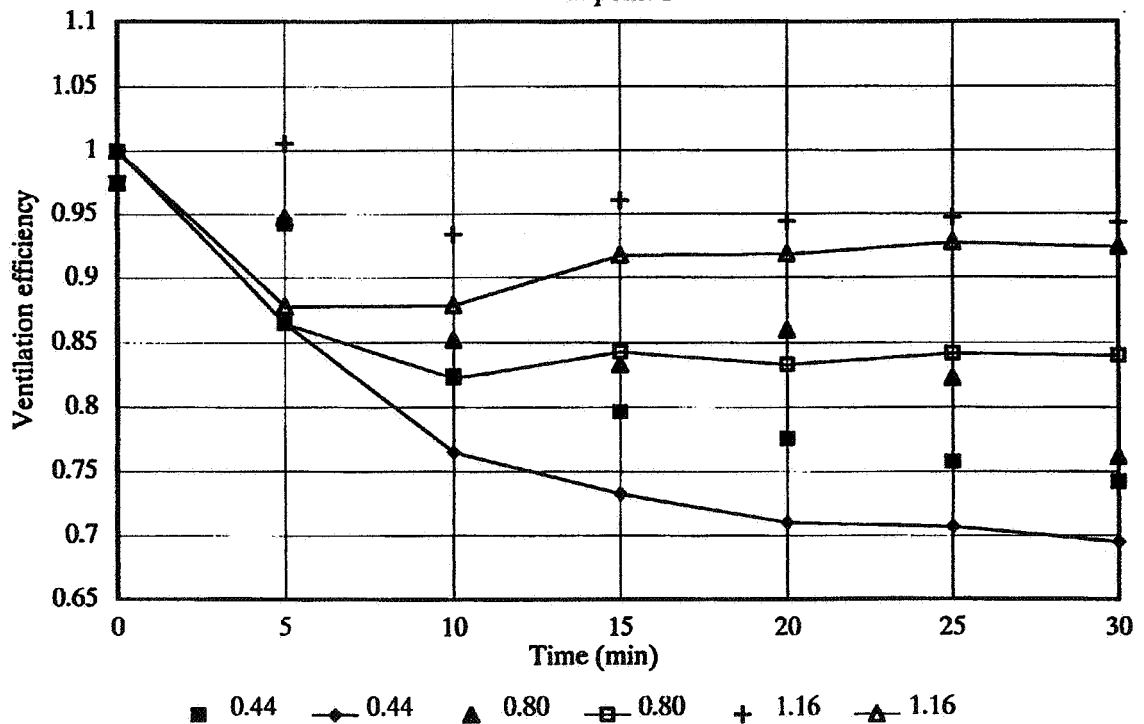
Case B1

**Fig. 5 – Calculated Concentration decay**  
at point 0



Case B1

**Fig. 6 – Meas. vs. calc. ventilation efficiency**  
at point 1



Case B1

Fig. 7 – Calculated concentration field

At time t = 10' – Case B3

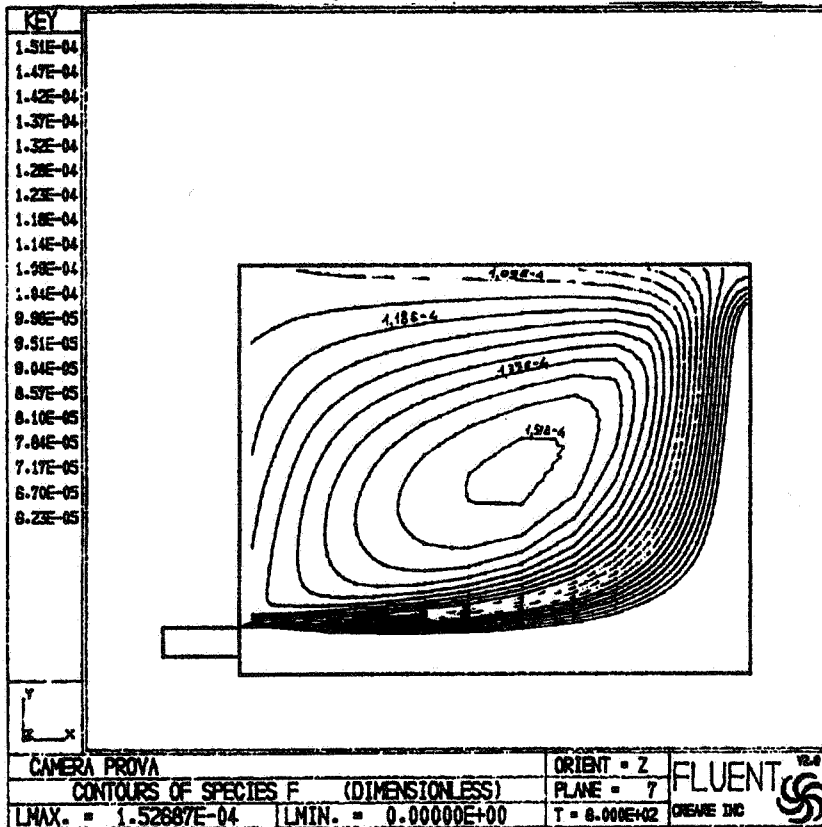


Fig. 8 – Calculated concentration field

At time t = 10' – Case C3

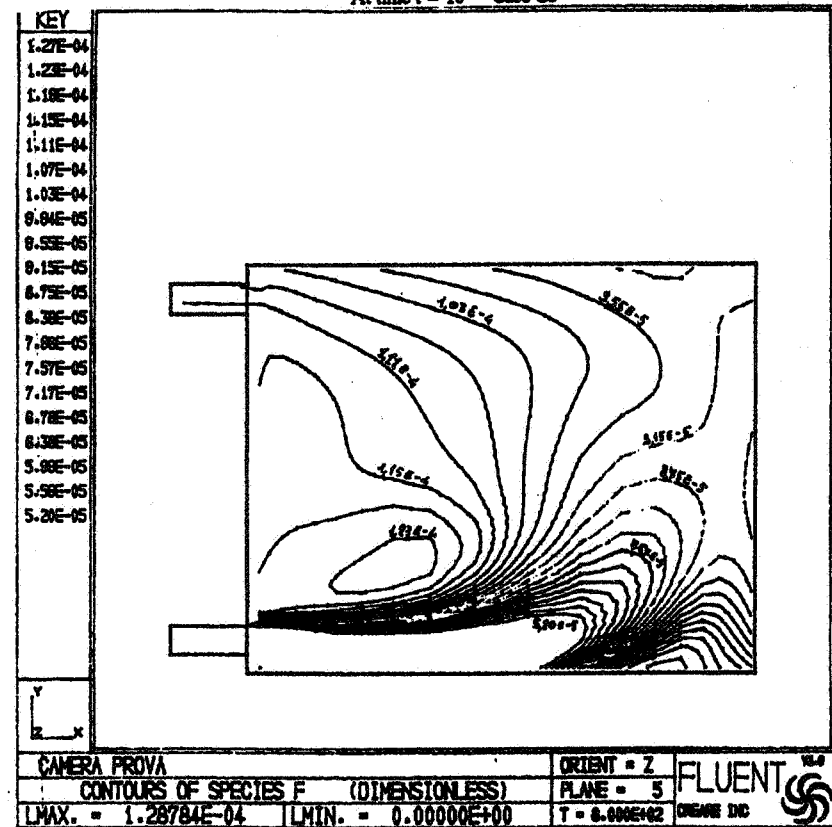


Fig. 9 – Calculated velocity field

At time  $t = 10^7$  – Case B3

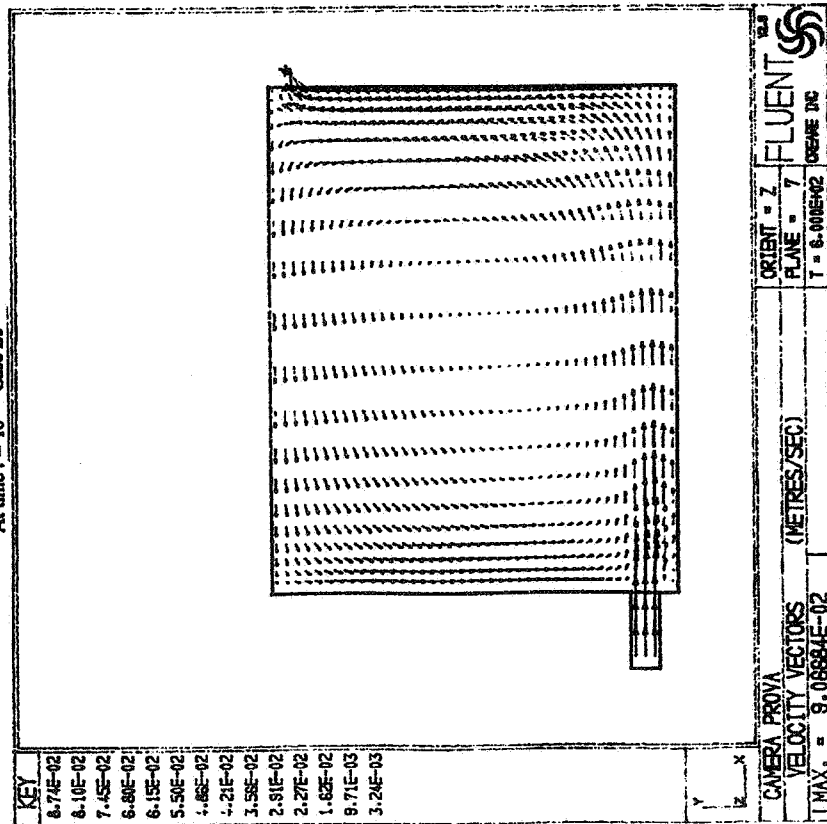


Fig. 10 – Calculated velocity field

At time  $t = 10^7$  – Case B1

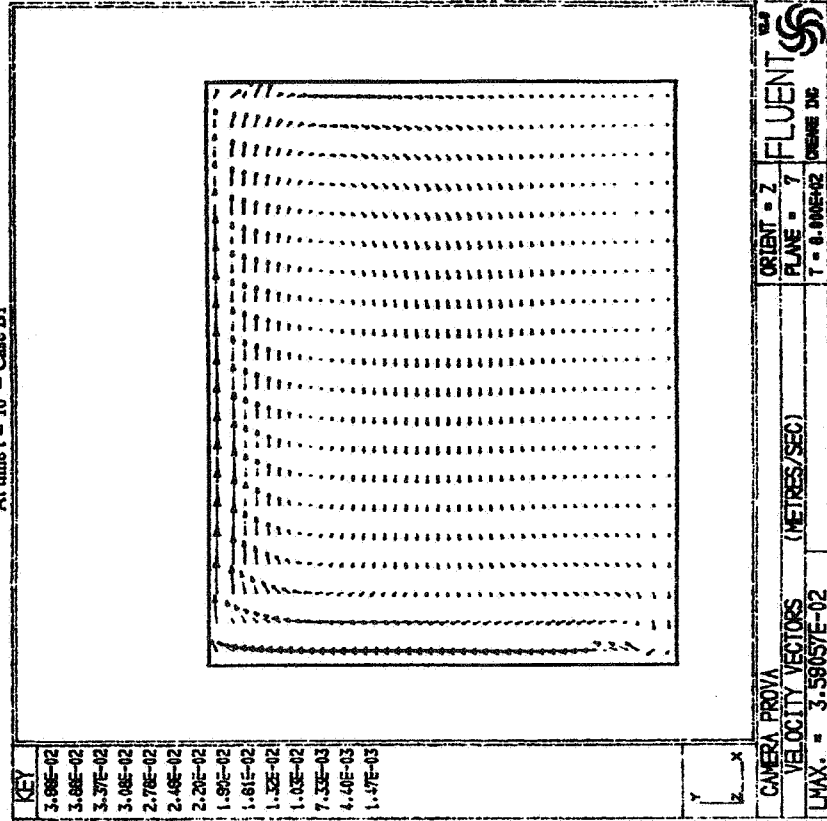


Fig. 11 – Measured concentration growth  
at point 7

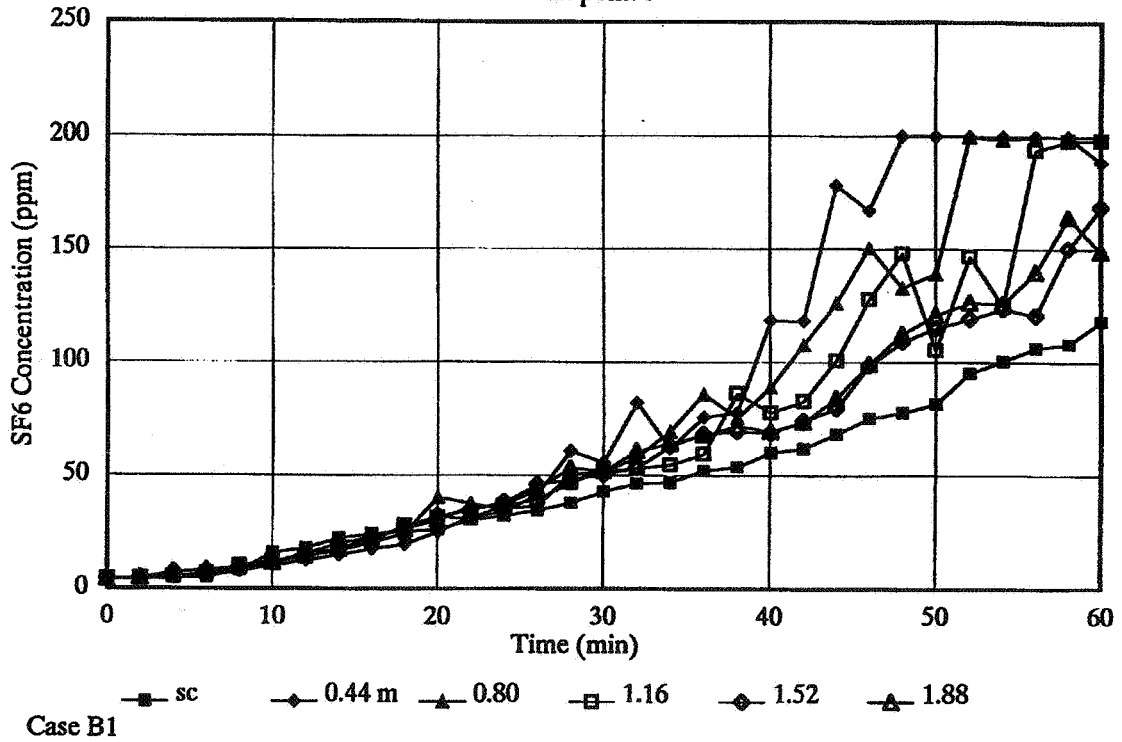


Fig. 12 – Calculated concentration growth  
at point 7

